RSC Advances

This is an *Accepted Manuscript*, which has been through the Royal Society of Chemistry peer review process and has been accepted for publication.

Accepted Manuscripts are published online shortly after acceptance, before technical editing, formatting and proof reading. Using this free service, authors can make their results available to the community, in citable form, before we publish the edited article. This *Accepted Manuscript* will be replaced by the edited, formatted and paginated article as soon as this is available.

You can find more information about *Accepted Manuscripts* in the **Information for Authors**.

ROYAL SOCIETY
OF **CHEMISTRY**

www.rsc.org/advances

Microphase Separated Sepiolite-Based Nanocomposite Blends of Fully Sulfonated Poly(ether ketone)/ Non-sulfonated Poly(ether sulfone) as Proton Exchange Membranes from Dual Electrospun Mats

Maryam Oroujzadeh, Shahram Mehdipour-Ataei*, Masoud Esfandeh

Iran Polymer and Petrochemical Institute, P.O.Box 14965/115, Tehran, Iran

Abstract

In this article nanocomposite blends of fully sulfonated poly(ether ketone) (PEK) and non-sulfonated poly(ether sulfone) (PES) were prepared from dual electrospinning process. Sepiolite was used as nanoparticle and just dispersed in non-sulfonated PES matrix to avoid barrier effects of nanoparticles against proton in these proton exchange membranes. As a novel and special technique, using dual electrospinning process and melting just non-sulfonated sepiolite dispersed fibers resulted membranes in which ionic paths (fibers of fully sulfonated PEK) were embedded in a sepiolite dispersed non-ionic matrix. The presence of these ionic channels was proved by stained transmittance electron microscopy (sTEM). Thermal and mechanical properties and also water absorption, dimensional stability, and proton conductivity of these hydrophilic/hydrophobic phase separated membranes were measured and investigated in different sepiolite and sulfonated fiber contents.

Keywords: proton exchange membranes, electrospinning, poly(ether ketone), poly(ether sulfone), sepiolite.

1. Introduction

Recently, introduction of nanoparticles in proton exchange membranes has attracted a lot of attentions and a great number of inorganic nanoparticles in different shapes and types have been tried.[1,2] Generally, targets of adding nanoparticles to the polymeric matrix of proton exchange membranes are improving mechanical strength, dimensional and thermal stability of the membrane, and also decreasing the water absorption and methanol permeability (for direct methanol fuel cells) of prepared membranes.[3-5] However, this strategy suffers from some disadvantages. One of the main drawbacks of

using nanoparticles in proton exchange membranes is that nanoparticles act as a physical barrier against proton transportation and decrease proton conductivity of resulted membrane.[6-8]

On the other hand, the challenge to finding an alternative membrane for Nafion in fuel cell applications is widely increasing because of some disadvantages of Nafion membranes such as its instability at temperature above 80 °C or its high methanol crossover in direct methanol fuel cells.[9-13] Nevertheless, in most of introduced alternative polymers, the proton conductivity values were not the same as the proton conductivity of Nafion membranes that is attributed to the difference between microstructure of Nafion membranes and alternative aromatic polymers. It has been proved that separated hydrophilic/ hydrophobic microstructure in Nafion membranes is larger than other alternative aromatic polymers and this is the main reason of improved efficiency of proton transfer in Nafion membranes.[14] So, different techniques have been used to improve the microphase separation and consequently the proton conductivity of these alternative membranes like synthesis of block copolymers or polymers with accumulations of sulfonic acid groups in some parts of the chain.[15-24]

In the present research two main purposes were followed by the authors. The first one is formation of hydrophilic/hydrophobic separated regions in the structure of proton exchange membrane by producing ionic paths in totally hydrophobic matrix from novel technique using dual electrospinning. In electrospinning process, an electrical charge is used to draw submicron fibers from a polymeric solution with specific concentration and in dual electrospinning process, two polymeric solutions are electrospun simultaneously.

The other is introducing inorganic nanoparticles into the membranes structure in such a way that no negative effect on proton conductivity of resulted membranes occur. Sepiolite was used as a nanoparticle in this investigation. Sepiolite is a fibrous magnesium silicate with the unit cell formula of $Si_{12}O_{30}Mg_8(OH)_4(H_2O)_4 \cdot 8H_2O$ and a large surface area.[25, 26]

The base polymers of blend membranes in this investigation were fully sulfonated PEK and non-sulfonated PES both synthesized in our laboratory. Membranes were prepared by dual electrospinning of two mentioned polymers. For introducing sepiolite nanoparticles into polymeric matrix, they were dispersed in the solution of non-sulfonated PES before electrospinning process. Then this nano-dispersed solution of non-sulfonated PES and fully sulfonated PEK were electrospun simultaneously.

In this way, electrospun mats consisted of fully sulfonated PEK fibers and non-sulfonated PES fibers containing dispersed nanoparticles were prepared. Due to the presence of sulfonated groups in every repeating unit of fully sulfonated PEK fibers, the two mentioned polymeric fibers had quite different melting points. This difference resulted from the fact that ionic structure increases the melting or softening point of sulfonated PEK in comparison to non-sulfonated PES fibers. By applying hot-press at certain temperature, the fibers of non-sulfonated PES containing nanoparticles were melted and covered the fully sulfonated fibers of PEK as a matrix. So, nanocomposite blend proton exchange membranes composed of ionic channels of PEK in PES matrix containing sepiolite nanoparticles were resulted.

2. Experimental

2.1. Materials

4,4′-Difluorobenzophenone (DFB) and bis-(4-chlorophenyl sulfone) (BCPS) as dihalide monomers (both from Aldrich) recrystallized from toluene before use. 4,4′-(1,4-Phenylene diisopropylidene) bisphenol (PBP) as dihydroxy monomer (from Aldrich) recrystallized from xylene. Potassium carbonate (from Merck) was dried at 120 °C in a vacuum oven overnight. Dimethyl acetamide (DMAc) (from Merck) was dried over calcium hydride for 12 h and then distilled under reduced pressure and stored over molecular sieves. Ethanol, toluene, xylene, tetrahydrofuran (THF), dimethylformamide (DMF), 2-propanol, fuming sulfuric acid (30%) (All from Merck) were used as received.

2.2. Synthesis of sulfonated monomer and related sulfonated and non-sulfonated polymers

Synthesis of sulfonated DFB and PEK, was performed according to procedure reported previously.[27]

Condensation polymerization of sulfonated DFB (sDFB) as dihalide monomer and PBP as dihydroxy monomer resulted fully sulfonated PEK. Non-sulfonated PES was synthesized from condensation polymerization of BCPS as dihalide and PBP as dihydroxy monomers. Both condensation polymerizations were performed in the presence of potassium carbonate in DMAc and toluene as solvents. A representative procedure for synthesis of non-sulfonated PES was as follows:

1.4358 g of BCPS and 1.7323g of PBP were added to a three necked flask equipped with a nitrogen inlet and a Dean-Stark trap. After adding 16 ml of DMAc and 8 ml of toluene, the mixture was heated to 140 °C. The mixture was refluxed for 4 h and then the temperature was raised to 175 °C until completing the reaction. After that, the resulted viscous non-sulfonated PES was poured into excess amounts of deionized water after dilution with DMAc and stirred for 24 h to remove any remained salts. Then, the resulted fibrous polymer was dried at 120 °C in a vacuum oven.

2.3. Dispersion of sepiolite nanoparticles in non-sulfonated PES solution

Non-sulfonated PES was dissolved in 50:50 mixture of DMF/THF as solvent (10 wt%) then specific amounts of sepiolite nanoparticles were added to the solution. After 20 minutes stirring and then 20 minutes sonication of the solution in an ice bath, the nanoparticle dispersed solutions were prepared for electrospinning. Two solutions with concentrations of 4 and 8 wt% nanoparticles in non-sulfonated PES polymer were prepared in this step.

2.4. Dual electrospinning of synthesized polymers

Sepiolite dispersed non-sulfonated PES solution and fully sulfonated PEK solution were electrospun simultaneously. To prepare proper fibers and mats in electrospinning process, various solvents were tested and as mentioned above 50:50 mixture of DMF/THF for non-sulfonated PES, and DMF for fully sulfonated PEK were selected.

Other electrospinning parameters like concentration of polymer solutions, flow rates, applied voltage, needle to collector distance, and collector rotation speed were optimized for both fully sulfonated PEK and sepiolite dispersed non-sulfonated PES to find the best conditions for producing fibers with no beads or defects. As a result, for dual electrospinning of 10 wt% of nanoparticle dispersed non-sulfonated PES in 50:50 mixture of DMF/THF, and also electrospinning of 25 wt% of fully sulfonated PEK in THF the other parameters were as follows: applied voltage of 27 kV, needle to collector distance of 15 cm, collector rotating speed of 700 rpm, and collector reciprocal motion speed of 8.8 mm/s. However, the flow rates for fully sulfonated PEK and non-sulfonated PES polymer solutions were 0.2-0.3, and 0.9-1.3 ml/h, respectively. Each sample was electrospun for 4.5 h.

For preparing mats with different degrees of fully sulfonated PEK fibers, two series of mats with 35 and 55 wt% of sulfonated fibers and each series with two different contents of nanoparticles (4 and 8 wt%) were prepared. For comparison, two mats without any sepiolite nanoparticles were also prepared. In this way, 6 series of mats were electrospun in this investigation.

2.5. Processing of the electrospun mats

As shown schematically in Figure 1, the porous structure of mats prepared from dual electrospinning process (Figure 1a) was converted to the suitable proton exchange membranes for fuel cell applications via the following procedure: Firstly, blend nanocomposite mats compressed under pressure of 125 kg/cm^2 for 10 seconds at room temperature made packed fiber mats (Figure 1b). In this step the thickness of mat reduced to half. Then, these compressed mats were hot-pressed at the pressure of 125 kg/cm^2 and temperature of 220 °C for 15 seconds (Figure 1c). This step was repeated three times with rotating the mats. Using this method, the fibers of non-sulfonated PES containing sepiolite nanoparticles were melted and flowed between fully sulfonated PEK fibers via hot-pressing without damaging the sulfonated fibers structure. Heat and pressure in this step just caused fusion between fully sulfonated PEK fibers and resulted in an interconnected network for proton transportation. By

dispersing the sepiolite in non-sulfonated solution and hot-pressing the electrospun mats, nanoparticles were just dispersed in non-sulfonated matrix without entrance to the fully sulfonated fibers. So, using nanoparticles in this way had no negative effect on proton conductivity of final membranes. Finally six series of membranes with different contents of fully sulfonated PEK fibers (35 and 55 wt%) and different contents of sepiolite nanoparticles (4 and 8 wt%) were prepared in this way. It should be noted that unlike other previously reported studies of fuel cell applications in which electrospinning process was just used as a technique for preparing membrane or hybrid membranes,[28-34] in this research the process was used as a procedure to induce separated hydrophilic/hydrophobic regions in the structure of membrane.
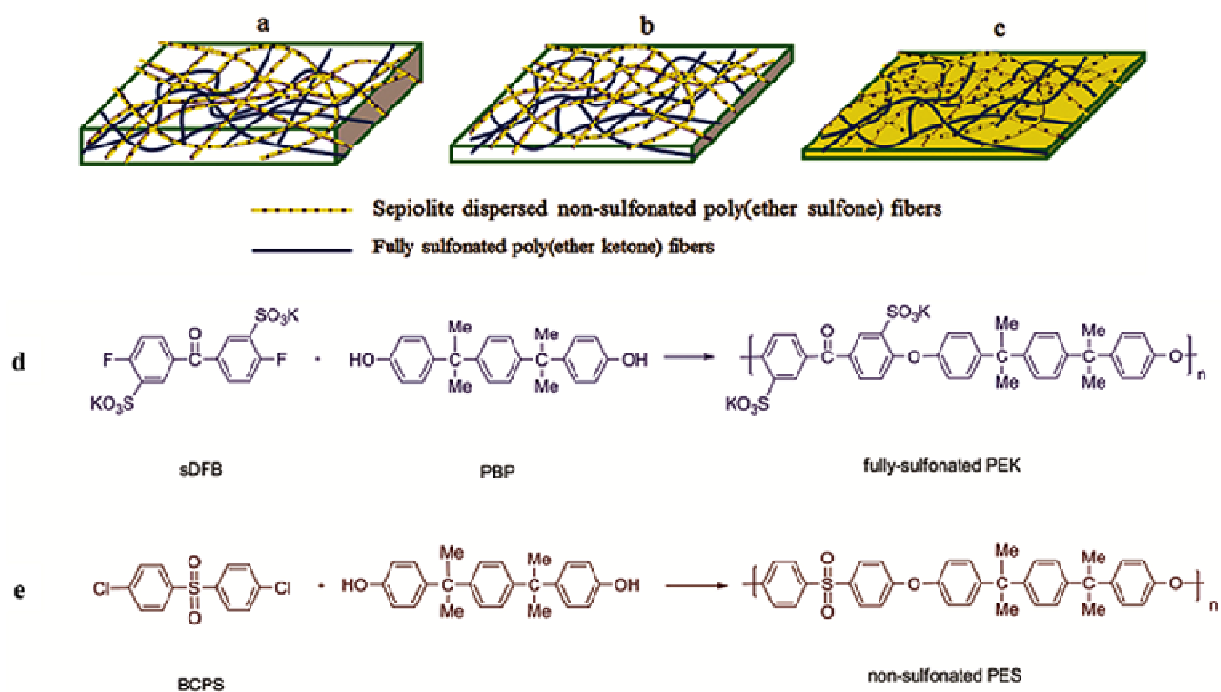

Figure 1. Schematic representation of prepared electrospun mats (a), mats after pressing (b), and membranes after hot-pressing (c), and also Synthesis of fully-sulfonated PEK (d) and non-sulfonated PES(e)

The final step in preparing these blend nanocomposite membranes was converting the sulfonate groups from salt to acid form in PEK fibers. To achieve this, membranes were immersed in 4 M H_2SO_4 solution for 24 h to convert potassium salt form of ionic groups of PEK fibers to the sulfonic acid groups. Then membranes were immersed in deionized water for 24 h to wash the excess acid. Afterwards all membranes were vacuum dried at 60 °C for 12 h.

2.6. Measurements

For characterization of sulfonated monomer (sDFB), ^{1}H-NMR (Bruker Avance DPX 400MHz) and FT-IR (Bruker- IFS48) spectroscopy were used and the results were reported previously.[27] The structure of fully sulfonated PEK and non-sulfonated PES was also confirmed with FT-IR spectroscopy.

The number average molecular weights of the synthesized sulfonated PEK and PES were determined by gel permeation chromatography (GPC- Waters chromatograph) with polystyrene standards in DMF and also THF as eluent.

Thermogravimetric analysis (TGA) from room temperature to 650 °C at a heating rate of 10 °C/min in air atmosphere was performed with a Mettler TGA/DSC 1 used to determine the thermal stability of prepared membranes.

Scanning electron microscopy (SEM) was applied to study the morphology of electrospun fibers and prepared mats using a VEGA TESCAN at an accelerating voltage of 20 kV. Elemental map of Si was used to study the probability of the presence of nanoparticles agglomerations by performing Energy dispersive X-ray Analysis (EDXA).

Transmittance electron microscopy (Philips S-208TEM microscope) was used to confirm the presence and dispersion of sepiolite nanoparticles in nanocomposite blend membranes. Also, stained TEM method was used to approve the existence of fully sulfonated PEK as fibers after hot-pressing step. For staining the samples, $AgNO_3$ solution was used.

Ion exchange capacity (IEC) of membranes was determined via routine titration method. 0.06 g of membrane samples were immersed in 2 M NaCl solution for 24 h. After replacing H^+ ions with Na^+, the liberated H^+ ions were titrated by 4 mM NaOH solution. Phenolphthalein was used as indicator for titration and at least three measurements were performed for each sample. The following equation was used to calculate the IEC values:

$$IEC = \frac{V_{NaOH} \times M_{NaOH}}{\text{weight of dry sample}}$$

Where, V_{NaOH} and M_{NaOH} are the volume and concentration of NaOH solution, respectively.

Water absorption of prepared membranes was measured as the increase in weights of dry samples after immersing them in deionized water for 24 h. To pursuing the amounts of water absorption during the time, the test continued for 750 h. The following equation was used for determination of water absorption values:

$$\textit{water absorption } (\%) = \frac{W_w - W_d}{W_d} \times 100$$

Where, W_w and W_d are wet and dry weights of membrane samples, respectively.

Dimensional stability of nanocomposite blend membranes was measured from swelling ratio of membranes. The length of samples in dry and wet states was determined and their swelling percent were calculated by the following equation:

$$\textit{swelling } (\%) = \frac{L_w - L_d}{L_d} \times 100$$

Where L_d is the length of dry membrane and L_w is the length of membrane in wet state.

The proton conductivity measurements were performed by electrochemical impedance spectroscopy (EIS) in a homemade cell using Autolab PGSTAT 30 with AC amplitude of 50 mA ranging from 1 to 10^6 MHz in lateral direction at room temperature and also 80 °C in water. The nanocomposite blend membranes were fully hydrated for 24 h before measurements. The resistance of the membrane was

taken at the frequency that produced the minimum imaginary response. The proton conductivity was calculated using the following equation:

$$\sigma = \frac{L}{RA}$$

In which, L is the distance between two electrodes, R is the membrane resistance and A is the membrane cross-sectional area.

The mechanical strength of membranes was determined from tensile test by a STM-20 according to ASTM-D 882 at the speed of 5 mm/min at room temperature. 50 mm × 10 mm rectangular samples were used. At least 3 samples were tested for each measurement. To study the effect of hydration on mechanical properties, tensile strength of the membranes after 24 hours immersion in water were measured as well.

3. Results and discussion

3.1. Synthesis and characterization of sulfonated monomer, fully sulfonated PEK, and non-sulfonated PES

sDFB as sulfonated monomer was synthesized via electrophilic aromatic sulfonation reaction that was reported previously. FT-IR and ^{1}H-NMR spectroscopy confirmed successful synthesis of monomer and its purity.[27]

Fully sulfonated PEK and non-sulfonated PES polymers were synthesized using condensation polymerization of stoichiometric amounts of sDFB as dihalide and PBP as diol monomers (Figure 1d), and also BFPS and PBP monomers (Figure 1e), respectively.

FT-IR spectroscopy approved the structure of synthesized polymers. Characteristic bands for non-sulfonated PES at 1160 and 1323 cm^{-1} were observed attributed to sulfone functional groups. For fully sulfonated PEK, peaks at 1029 and 1085 cm^{-1} were observed related to sulfonic acid groups and also characteristic band for carbonyl group at 1661 cm^{-1} was observed. Characteristic bands for ether

linkages and aliphatic hydrogens at 1246 and 2967 cm^{-1}, respectively were observed for both polymers[35].

Gel permeation chromatography was used to determine the number average molecular weights to confirm the successful synthesis of polymers. As a result, the number average molecular weights for fully sulfonated PEK and non-sulfonated PES were 58.000 and 83.000 g/mol, respectively.

3.2. Thermal properties of nanocomposite blend membranes

The presence of pendent sulfonic acid groups along the polymer chain decreases thermal stability of polymers because of the lower heat-resistance properties of these groups[36]. So, as depicted in Figure 2, increasing the sulfonic acid contents from sample B-35 to sample A-55 decreased the amount of T_5% (temperature for 5% weight loss in polymer) (Table 1). Nevertheless, from results shown in Table 1, adding nanoparticles to the blend membranes in both sulfonation degrees of 35% and 55% led to more thermally stable membranes. Sepiolite nanoparticles acted as insulator and mass transport barrier in decomposition of polymer matrix and this phenomenon was observed for 4wt% sepiolite in both sulfonation contents of 35 and 55% although there were significant difference between thermal stability of 4 or 8 wt% sepiolite contents in nanocomposite blend membranes[37]. Both sulfonated polymer (35 and 55%), nanocomposite membranes with 4 wt% sepiolite showed better thermal stability in comparison to nanocomposite samples with 8wt% sepiolite. This observation could be attributed to agglomeration of nanoparticles in higher contents of sepiolite (shown in Figure 5). It should be mentioned that all membranes showed four steps of weight losses. The first one was related to dehydration of samples and next three weight losses were attributed to the decomposition of sulfonated and non-sulfonated polymer chains. Liberation of sulfonic acid groups from fully sulfonated PEK at about 250 °C, elimination of methyl groups from structure of both polymers, and decomposition of polymer backbone were related to second, third, and last weight losses, respectively.

RSC Advances

Table 1. IEC and $T_{5\%}$ of nanocomposite blend membranes

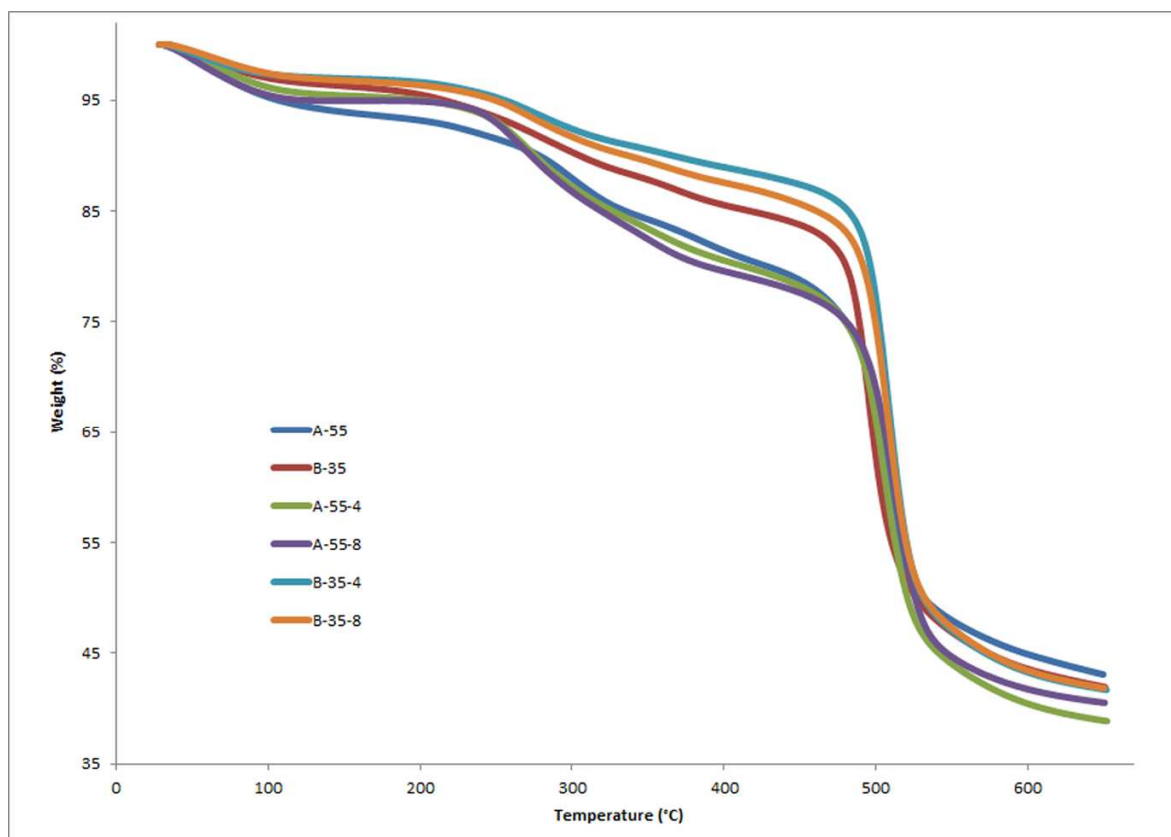| Nanocomposite blend samples	Sulfonated polymer content (wt%)	Sepiolite content (wt%)	IEC (meq/g)	$T_{5\%}$ (°C)
A-55	55	-	1.26	106
B-35	35	-	0.72	214
A-55-4	55	4	1.28	199
A-55-8	55	8	1.24	121
B-35-4	35	4	0.73	255
B-35-8	35	8	0.75	249
Nafion 115	-	-	0.91	290

Figure 2. TGA curves of nanocomposite blend samples

3.3. Morphology of membranes and dispersion of sepiolite nanoparticles in membranes

To study the morphology of prepared fibers from electrospinning process and also the morphology of

mats and final membranes, scanning electron microscopy was used. The distribution of fibers diameter

was analyzed by ImageJ. At least 50 fibers were randomly selected for the measurement. The results showed that the average fiber diameter was 214 nm.

As shown in Figure 3a, there was uniform distribution of both types of fully sulfonated and non-sulfonated fibers. The photograph of electrospun mat was also represented in photograph of Figure 3a. As expected, the mat was not transparent and because of completely porous structure it was not suitable for using as proton exchange membranes. To convert the porous mats to the non-porous and defect-free membranes, the mats were pressed in the next step to produce physical connection between fibers (Figure 3b). As shown in photograph of Figure 3b, densification of fibers by pressing reduced the thickness of the mat and converted it to a translucent mat. The last step was hot-pressing the mats. After hot-pressing and as shown in Figure 3c, sepiolite dispersed non-sulfonated PES fibers were melted and flowed between fully sulfonated PEK fibers. As depicted in photograph of Figure 3c, a completely transparent membrane was prepared.
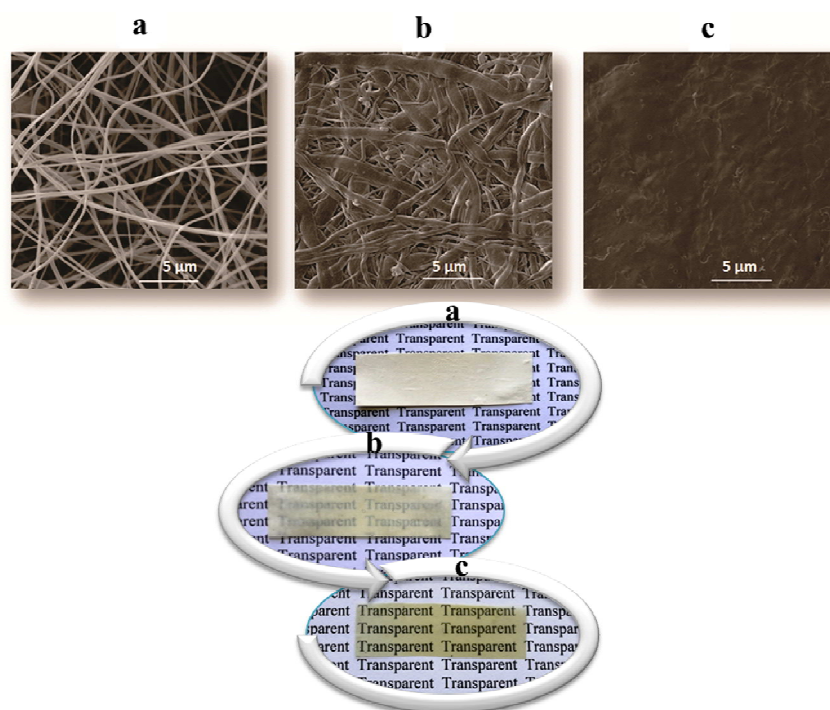

Figure 3. SEM images and Photographs of electrospun mat (a), mats after pressing (b), and membranes after hot-pressing (c)

To prove the presence of fully sulfonated PEK as fibers after hot-pressing step and also the presence of ionic channels in final membranes, stained TEM technique was used. For staining the membranes, the hydrogen atoms of sulfonic acid groups were replaced with Ag^+ ions by immersing the samples into $AgNO_3$ solution before preparation of samples for TEM. The TEM image of the stained sample (surface and cross section) represented in Figure 4 (a,b). As shown in the Figure 4a, the presence of fibrous structures in the matrix of non- sulfonated PES was completely clear. So, final membranes after hot-pressing stage contained fully sulfonated polymer as fibers in a non-sulfonated matrix or in other words, ionic channels in a non-ionic matrix. So in this way the efficiency of this technique for preparing hydrophilic/hydrophobic phase separated structures in these proton exchange membranes was approved. The cross sectional image of the final membrane was shown in Figure 4b. The cross section of fully sulfonated fibers (ionic channels) and distribution of them in this image was observable.
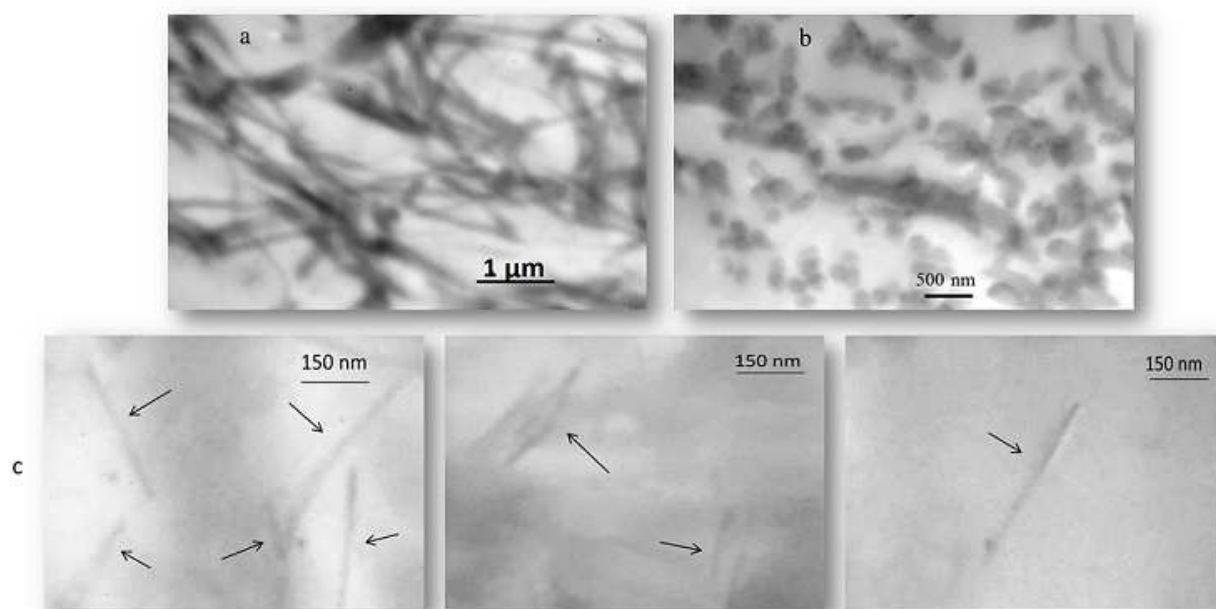
Figure 4. Stained TEM images of surface (a) and cross section (b) of final sample of A-55-4 after hot-

pressing stage, and TEM images from dispersion of sepiolite nanoparticles in A-55-4 sample. Arrows

show sepiolite nanoparticles

Dispersion of sepiolite nanoparticles in non-sulfonated PES matrix was also approved by TEM (Figure

4c) shows the data. According to the Figure, suitable dispersion of sepiolite nano-fibers and rare

aggregates was deduced. This observation showed that using ultrasonic probe as well as the applied

shear to the sepiolite nanoparticles in electrospinning process caused good dispersion of sepiolite

nanofibers. Si mapping used to study the agglomeration of nanoparticles. As shown in Figure 5, for the

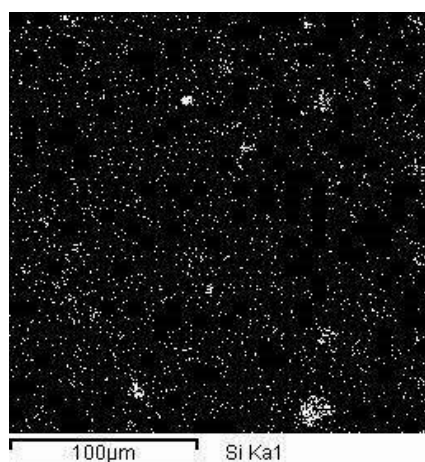sample A-55-8 some agglomeration of sepiolite nanoparticles can be seen.

Figure 5. Si mapping for A-55-8

3.4. Ion exchange capacity, water absorption and swelling ratio measurements

In proton exchange membranes, IEC is defined as the number of sulfonic acid groups per gram of

membranes. It should be noted that the IEC value of synthesized fully sulfonated PEK was 2.9 meq/g.

By optimizing the electrospinning rate of fully sulfonated PEK solution and molar ratio of PEK and

PES solutions, two series of nanocomposite blend membranes with sulfonated fiber contents of 35 and

55 wt% were prepared using fully sulfonated PEK to non-sulfonated PES molar ratios of 0.55 and 1.2,

respectively. The measured IEC value for 35 wt% samples was in the range of 0.72-0.75 meq/g and for

55 wt% samples was in the range of 1.24-1.28 meq/g. As expected and showed in Table 1, the IEC values for all A-membranes (55 wt%) and also all B-membranes (35 wt%), with or without sepiolite nanoparticles, were almost the same. Small differences could be attributed to the measurement errors or small instabilities in electrospinning rates of polymeric solutions related to the electrospinning apparatus. To ensure whether the presence of sulfonated fibers inside the totally hydrophobic PES matrix prevents release of SO_3^- ions or not, the IEC tests were repeated after five days of immersion of membranes in NaCl solution for all nanocomposite blend membranes. The same results were obtained from these measurements.

Water absorption measurements showed that from B-samples to A-samples by increasing the IEC value, water absorption increased. This observation was attributed to increasing the fully sulfonated fiber contents from 35 to 55 wt%. Another observation from results listed in Table 2 was decreasing the water absorption of nanocomposite membranes in comparison to samples with no sepiolite contents (A-55 and B-35) and also decreasing the water absorption of nanocomposite samples with 8 wt% sepiolite content (A-55-8 and B-35-8) compared to 4 wt% samples (A-55-4 and B-35-4) in both contents of sulfonated fibers. This observation could be explained simply by the barrier effects of nanoparticles that led to the decrease in water absorption of samples. Contrary to the expectations and unlike previous reports for microphase separated samples,[38-41] all results showed that although in these membranes there were completely hydrophilic fully sulfonated fibers, the presence of hydrophobic matrix around these fibers kept the water absorption in acceptable range and smaller than water absorption of Nafion membranes even for membranes with higher IEC values (A-membranes) (Table 2).

Table 2. IEC values, Water absorption, swelling ratio, and proton conductivity of nanocomposite blend membranes and Nafion 115

Nanocomposite blend samples	IEC (meq/g)	Water absorption (%)	Swelling ratio (%)	Proton conductivity (25 °C)	Proton conductivity (80 °C)
A-55	1.26	19.2	3.22	0.097	0.270
B-35	0.72	4.5	1.20	0.042	0.102
A-55-4	1.28	18.4	2.8	0.106	0.280
A-55-8	1.24	15.8	1.11	0.095	0.275
B-35-4	0.73	4.3	0.85	0.046	0.132
B-35-8	0.75	4.2	0.33	0.057	0.133
Nafion 115	0.91	32.6	8.15	0.085	0.108

To explore dimensional stability of nanocomposite blend membranes, the swelling ratios of membranes were measured. As noted in Table 2, for swelling ratios also the same trend was observed. By increasing the IEC values of membranes the swelling ratio was increased, also increasing the sepiolite contents in both A- and B-membranes caused a reduction in swelling ratio of membranes. Moreover, all of membrane samples showed lower swelling ratio compared to Nafion membrane which was attributed to the presence of non-sulfonated hydrophobic matrix. Since the hydrophilic fibers were covered by hydrophobic matrix, swelling ratio like water absorption values were kept in suitable range compared to Nafion membrane (Table 2). For following the trend of water absorption and swelling ratio of membranes these measurements were continued for 750 h and the test was carried out several times during the period. The results for swelling ratio and water absorption were plotted in Figure 6 (bottom) and Figure 6 (up), respectively.

As shown in Figure 6 (bottom), the highest swelling ratio of membranes was observed in first 24 h and after that it remained almost constant. However, the swelling ratio of membranes in all contents of fully sulfonated fibers and also all contents of sepiolite nanoparticles were under 4% which was desirable for fuel cell application. Moreover, for water absorption values, shown in Figure 6 (up), for all A-membranes with fully sulfonated contents of 55 wt%, the increasing trend was continued during this

16

time with small rates. On the other hand, in B-membranes with 35 wt% contents of fully sulfonated fibers, the water absorption remained almost constant during the test time. This observation showed that there might be a threshold limit for the content of fully sulfonated fibers in hydrophobic matrix after that, the hydrophobic matrix cannot prevent the excessive water absorption of membranes. Nevertheless, all nanocomposite blend membranes of this investigation showed acceptable water absorption degrees compared to other previously reported membranes with hydrophilic/hydrophobic microphase separated structures[38, 42].
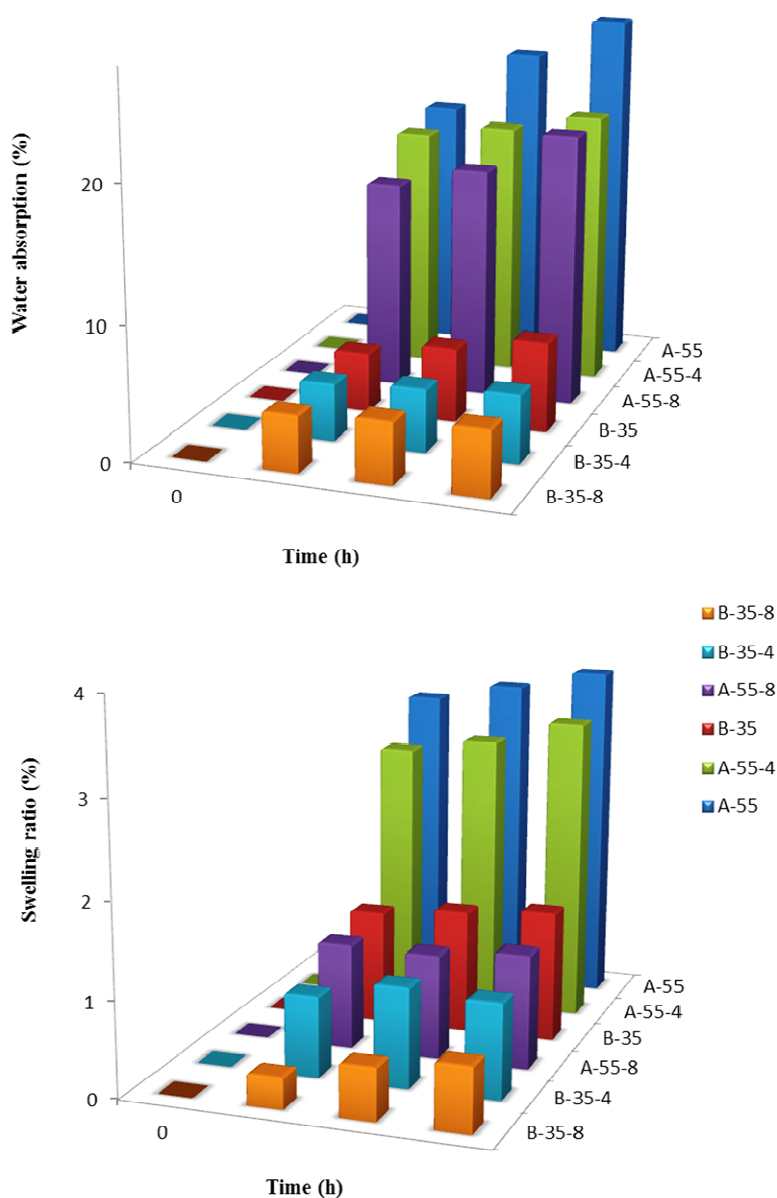
Figure 6. Water absorption (up) and Swelling ratio (bottom) of membranes as a function of time

3.5. Proton conductivity of prepared membranes

Proton conductivity of all membranes was measured at 25 and 80 °C and results were listed in Table 2. As expected and according to the results, proton conductivity of all membranes was increased with increasing the IEC value or in other words by increasing the content of fully sulfonated PEK fibers from B- to A-membranes. Another expected result was increasing the proton conductivity of membranes with increasing the temperature from 25 to 80 °C which was attributed to the higher energy of conducting ions and lower resistance of membrane at higher temperatures.

Anyway as shown in Table 2, at given temperature the proton conductivity of all A-membranes and also all B-membranes were almost the same (with same IEC values). Small differences might be related to the small differences in IEC values. Meanwhile, because of the presence of sepiolite nanoparticles just in hydrophobic matrix, the presence of nanoparticles and also the contents of nanoparticles did not influence the proton conductivity of membranes. This trend was observed at both temperatures. Another conclusion was that the presence of ionic paths and producing hydrophilic/hydrophobic separated microstructure remarkably improved the proton conductivity of membranes. As reported in Table 2, the proton conductivity of Nafion membranes with the IEC value of 0.9 at 25 °C and 80 °C was 0.085 and 0.108 S/cm, respectively. The obtained results showed that the proton conductivity of B-membranes with average IEC value of 0.73 meq/g at higher temperatures was almost similar to Nafion membranes with IEC value of 0.9 meq/g that could be related to the presence of ionic paths. However, increasing the IEC value to 1.26 meq/g in A-membranes strongly increased the proton conductivity at both temperatures. Moreover, the amount of water absorption and swelling ratios of these nanocomposite blend membranes even in IEC value of 1.26 meq/g were smaller than Nafion membranes. It should be noted that, the base polymers of these blend membranes unlike Nafion

membranes were thermally stable polymers. Therefore these blend nanocomposite membranes could be considered as suitable alternatives for Nafion membranes.

3.6. Mechanical strength of prepared membranes

To study the mechanical strength of prepared membranes tensile test and stress-strain curves were used. The results were shown in Table 3. As it is clear from the results, tensile properties of all prepared membranes were acceptable. However, addition of nanoparticles to the polymeric matrix reduced tensile strength and elongation at break, and increased the Young's modulus of membranes which was attributed to inorganic nature of nanoparticles. By comparing the tensile properties of samples A-55 and B-35, it was found that increasing the amount of fully sulfonated fibers improved the tensile properties of membranes. The result could be related to increasing hydrogen bonding between chains with increasing the contents of sulfonic acid groups. Performing the test in hydrated condition, as represented in Table 3, showed that tensile strength and tensile modulus of membranes decreased in wet state whereas elongation at break for all membranes increased. The result can be explained by the fact that water molecules play the role of a plasticizer that soften the membrane and reduce the load carrying capability[43].

Table 3. Mechanical properties of blend nanocomposite membranes

Nanocomposite blend samples	Tensile strength (MPa)		Young's modulus (GPa)		Elongation @ break (%)	
	dry	wet	dry	wet	dry	wet
A-55	69.32	49.21	1.72	1.37	6.10	10.98
B-35	55.23	34.24	2.90	1.88	4.25	6.37
A-55-4	36.49	27.36	2.70	1.70	5.14	8.74
A-55-8	30.17	21.11	3.01	2.19	3.96	5.90
B-35-4	35.50	21.36	2.52	1.63	2.75	4.95
B-35-8	38.05	25.40	2.71	1.78	3.53	5.65
Nafion 115	35.50	24.90	0.26	0.19	210	315

4. Conclusions

In this work nanocomposite blends of fully sulfonated PEK and non-sulfonated PES based on sepiolite nanoparticles were prepared using a new method. In this method dual electrospinning process was used for preparation of membranes with separated hydrophilic (fully sulfonated PEK fibers)/hydrophobic (non-sulfonated PES matrix) structures. The sepiolite nanoparticles were introduced just to the non-sulfonated PES matrix to prevent any negative barrier effect of these nano-fibers against proton transportation. TEM and sTEM images approved dispersion of nanoparticles and also the presence of ionic paths in final membranes. The membranes showed acceptable thermal and mechanical properties. In spite of the presence of fully sulfonated PEK fibers in the structure of membrane, the water absorption and swelling ratios for these samples were lower (i.e. more hydrolytic stability) than Nafion membranes. The proton conductivity of membranes was excellent which was attributed to the presence of ionic paths in hydrophobic matrix. Nevertheless, the results showed that dispersion of sepiolite nanofibers in non-sulfonated PES matrix had no negative effect on proton conductivities so these values for nanocomposite blend membranes were almost the same as same blend membranes without any sepiolite nanoparticles.

Acknowledgement

RSC Advances Accepted Manuscript

References

1.   J. Wang, H. Bai, H. Zhang, L. Zhao, H. Chen and Y. Li, *Electrochim. Acta*, 2015, **152**, 443-455.

2.   E. A. Mistri and S. Banerjee, *RSC Advances*, 2014, **4**, 22398-22410.

3.   E. Abouzari-Lotf, M. M. Nasef, H. Ghassemi, M. Zakeri, A. Ahmad, Y. Abdollahi, *ACS Appl Mater Interfaces*, 2015, DOI: 10.1021/acsami.5b02268.

4.   A. Aslan and A. Bozkurt, *Solid State Ionics*, 2014, **255**, 89-95.

5.   N. V. Prabhu and D. Sangeetha, *Chem. Eng. J.*, 2014, **243**, 564-571.

6.   Y. Jun, H. Zarrin, M. Fowler and Z. Chen, *Int. J. Hydrogen Energy*, 2011, **36**, 6073-6081.

7.   Y. He, C. Tong, L. Geng, L. Liu and C. Lü, *J.Membr. Sci*, 2014, **458**, 36-46.

8.   P. Kalappa and J. H. Lee, *Polym. Int.*, 2007, **56**, 371-375.

9.   M. Oroujzadeh, S. Mehdipour-Ataei and M. Esfandeh, *Int. J. Polym. Mater. Polym. Biomater*, 2015, **64**, 279-286.

10.   L. Akbarian-Feizi, S. Mehdipour-Ataei and H. Yeganeh, *J. Appl. Polym. Sci.*, 2012, **124**, 1981-1992.

11.   L. Wang, J. Zhu, J. Zheng and S. Zhang, *RSC Advances*, 2014, **4**, 25195-25200.

12.   X. Xu, L. Li, H. Wang, X. Li and X. Zhuang, *RSC Advances*, 2015, **5**, 4934-4940.

13.   Y. Yang, H. Gao and L. Zheng, *RSC Advances*, 2015, **5**, 17683-17689.

14.   Y. Yang, A. Siu, T. Peckham and S. Holdcroft, *Fuel Cells I*, 2008, 55-126.

15.   T. A. Kim and W. H. Jo, *Chem. Mater.*, 2010, **22**, 3646-3652.

16.   M. S. Jung, T.-H. Kim, Y. J. Yoon, C. G. Kang, D. M. Yu, J. Y. Lee, H.-J. Kim and Y. T. Hong, *J. Membr. Sci,* 2014, **459**, 72-85.

17.   D. W. Shin, S. Y. Lee, C. H. Lee, K.-S. Lee, C. H. Park, J. E. McGrath, M. Zhang, R. B. Moore, M. D. Lingwood and L. A. Madsen, *Macromolecules*, 2013, **46**, 7797-7804.

18.   K. Matsumoto, T. Higashihara and M. Ueda, *Macromolecules*, 2009, **42**, 1161-1166.

19.　　S. Zhou and D. Kim, *Electrochim. Acta*, 2012, **63**, 238-244.

20.　　S. Takamuku and P. Jannasch, *Macromolecules*, 2012, **45**, 6538-6546.

21.　　S. Takamuku, E. A. Weiber and P. Jannasch, *ChemSusChem*, 2013, **6**, 308-319.

22.　　Y. Yao, Z. Lin, Y. Li, M. Alcoutlabi, H. Hamouda and X. Zhang, *Adv. Energy Mater*, 2011, **1**, 1133-1140.

23.　　S. Lu, X. Xu, J. Zhang, S. Peng, D. Liang, H. Wang and Y. Xiang, *Adv. Energy Mater,*, 2014, **4**, 1400842.

24.　　D. C. Villa, S. Angioni, S. D. Barco, P. Mustarelli and E. Quartarone, *Adv. Energy Mater*, 2014, **4**, 1301949.

25.　　H. Chen, H. Lu, Y. Zhou, M. Zheng, C. Ke and D. Zeng, *Polym. Degrad. Stab.*, 2012, **97**, 242-247.

26.　　M. Suárez and E. García-Romero, *Appl. clay sci*, 2012, **67**, 72-82.

27.　　M. Oroujzadeh, S. Mehdipour-Ataei and M. Esfandeh, *Eur. Polym. J.*, 2013, **49**, 1673-1681.

28.　　T. Tamura and H. Kawakami, *Nano Lett.*, 2010, **10**, 1324-1328.

29.　　J. B. Ballengee and P. N. Pintauro, *J. Membr. Sci*, 2013, **442**, 187-195.

30.　　J. B. Ballengee and P. N. Pintauro, *Macromolecules*, 2011, **44**, 7307-7314.

31.　　J. Choi, K. M. Lee, R. Wycisk, P. N. Pintauro and P. T. Mather, *Macromolecules*, 2008, **41**, 4569-4572.

32.　　R. Takemori and H. Kawakami, *J. Power Sources*, 2010, **195**, 5957-5961.

33.　　M. M. Hasani-Sadrabadi, I. Shabani, M. Soleimani and H. Moaddel, *J. Power Sources*, 2011, **196**, 4599-4603.

34.　　J. Zhao, W. Z. Yuan, A. Xu, F. Ai, Y. Lu and Y. Zhang, *React. Funct. Polym.*, 2011, **71**, 1102-1109.

35.　　C. K. Shin, G. Maier and G. G. Scherer, *J. Membr. Sci*, 2004, **245**, 163-173.

36.   C. Wang, B. Shen, H. Dong, W. Chen, C. Xu, J. Li and Q. Ren, *Electrochim. Acta*, in press.

37.   G. Nawn, G. Pace, S. Lavina, K. Vezzù, E. Negro, F. Bertasi, S. Polizzi and V. Di Noto, *ChemSusChem*, 2015, **8**, 1381-1393.

38.   H. Hu, M. Xiao, S. Wang and Y. Meng, *Int. J. Hydrogen Energy*, 2010, **35**, 682-689.

39.   H. Ghassemi, J. E. McGrath and T. A. Zawodzinski, *Polymer*, 2006, **47**, 4132-4139.

40.   S. Tian, Y. Meng and A. S. Hay, *J. Polym. Sci., Part A: Polym. Chem.*, 2009, **47**, 4762-4773.

41.   A. Roy, X. Yu, S. Dunn and J. E. McGrath, *J. Membr. Sci*, 2009, **327**, 118-124.

42.   D. W. Seo, Y. D. Lim, S. H. Lee, M. A. Hossain, M. M. Islam, H. C. Lee, H. H. Jang and W. G. Kim, *Electrochim. Acta*, 2012, **86**, 352-359.

43.   R. Solasi, Y. Zou, X. Huang, K. Reifsnider and D. Condit, *J. Power Sources*, 2007, **167**, 366-377.

Captions:

Figure 1. Schematic representation of prepared electrospun mats (a), mats after pressing (b), and membranes after hot-pressing (c), and also Synthesis of fully-sulfonated PEK (d) and non-sulfonated PES(e)

Figure 2. TGA curves of nanocomposite blend samples

Figure 3. SEM images and Photographs of electrospun mat (a), mats after pressing (b), and membranes after hot-pressing (c)

Figure 4. Stained TEM images of surface (a) and cross section (b) of final sample of A-55-4 after hot-pressing stage, and TEM images from dispersion of sepiolite nanoparticles in A-55-4 sample. Arrows show sepiolite nanoparticles
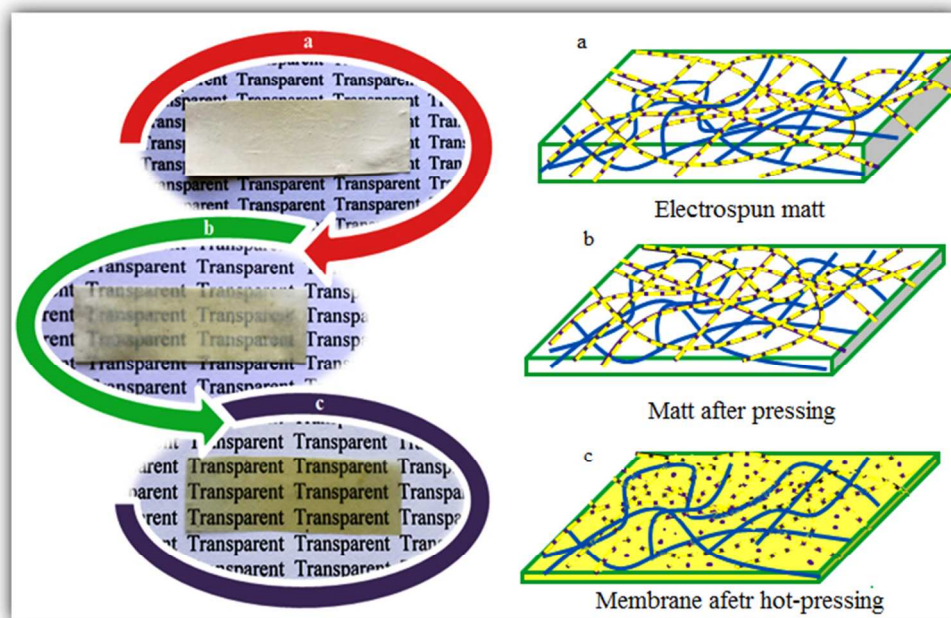
Figure 5. Si mapping for A-55-8

Figure 6. Water absorption (up) and Swelling ratio (bottom) of membranes as a function of time

Table 1. IEC and $T_{5\%}$ of nanocomposite blend membranes

Table 2. IEC values, Water absorption, swelling ratio, and proton conductivity of nanocomposite blend membranes and Nafion 115

Table 3. Mechanical properties of blend nanocomposite membranes

graphical abstract
196x130mm (96 x 96 DPI)